J Fluoresc (2013) 23:71–77
DOI 10.1007/s10895-012-1117-2

ORIGINAL PAPER

Immunoassays Based on Surface-Enhanced Fluorescence using Gap-Plasmon-Tunable Ag Bilayer Nanoparticle Films

Ruohu Zhang · Zhuyuan Wang · Chunyuan Song · Jing Yang · Asma Sadaf · Yiping Cui

Received: 13 May 2012 / Accepted: 30 July 2012 / Published online: 14 August 2012

Abstract A novel gap-plasmon-tunable Ag bilayer nanoparticle film for immunoassays is demonstrated. Different from a traditional Ag monolayer nanoparticle film, a desired number of polyelectrolyte (PEL) layers are deposited on the nanoparticles before the self-assembly of a second Ag nanoparticle layer. Interestingly, by controlling the number of the PEL interlayers, the gap plasmon between the two Ag nanoparticle layers can be tuned across the visible spectral range. The ability of the presented Ag bilayer nanoparticle films in fluorescence enhancement has been examined experimentally. A maximal enhancement of around 15.4 fold was achieved when 7 layers of polyelectrolyte were used. When this optimal Ag bilayer nanoparticle film was applied to fluorescence immunoassay, a performance with approximately 3.3-fold enhancement was obtained compared with that performed on a traditional glass substrate. The experimental results suggest that the presented gap-plasmon tunable Ag bilayer nanoparticle films have great potential in fluorescence-based immunoassays. The method of the bilayer-film construction presented here also provides new insights into the rational design of the plasmonic substrates.

Keywords Surface enhanced fluorescence · Surface plasmon resonance · Immunoassay · Ag nanoparticle · Substrate · Gap plasmon

Introduction

Fluorescence is one of the most powerful tools in medical and clinical diagnostics. Using fluorescence for detecting biomolecules, e.g., fluorescence immunoassay, has shown great potential [1]. However, there are some inherent limitations such as the low quantum yields and the poor photostabilities of the fluorophores. Surface enhanced fluorescence (SEF), to some degree, offers a solution to these issues [2–4].

When fluorophores are in close proximity to metallic nanostructures, generally within 5 to 20 nm [5–8], a number of appreciable effects take place, including an enhanced fluorescence, a decreased lifetime as well as an improved photostability [9]. The mechanism of SEF has been studied since the 1980s [10–12], and it is generally believed to be a combination of two processes: the enhancement of the excitation [13–15], and the enhancement of the emission, about the latter of which a model known as the radiating plasmon model (RPM) has been raised by Lakowicz [16], contributing a lot to the understanding of the SEF effect.

In the past decade, a number of reports that incorporated SEF into immunoassays can be found in the literature. Different silver nanostructures, either chemically grown [17], vapor deposited [18], or electrochemically prepared [19], were used as the substrate. One substrate with silver nanoparticles on an underlying metal film was found to be extremely effective for SEF and used in immunoassays with great signal enhancement [20]. Recently, a homogeneous silver nanoparticle substrate was developed, and significant improvements in sensitivity and limit of detection were obtained in the SEF-based immunoassay [21]. All those reports mainly focused on the design of the SEF substrate, which plays a key role in enhancing the excitation rate and/or emission rate of the fluorophores.

A substrate with both good homogeneity and appreciable SEF activity is favored in practical use. Generally, silver fractal-like substrates exhibit a significant enhancement but the homogeneity is less satisfactory [19]. Self-assembled metallic nanoparticles can be advantageous in homogeneity over traditional silver island films (SIFs) but are difficult to achieve

R. Zhang · Z. Wang · C. Song · J. Yang · A. Sadaf · Y. Cui (✉)
Advanced Photonics Center, Southeast University,
Nanjing 210096, People's Republic of China
e-mail: cyp@seu.edu.cn

a high surface density of nanoparticles, which strongly affects the enhancement [4]. Another issue involved in exploiting the SEF activity is the optimization of the SPR extinction spectrum of the substrate [22], which is of great importance for the supported plasmonic effects. Benefiting from the ever-improving synthetic chemistries, metallic nanoparticles with well-defined geometries and sizes have been successfully prepared, which can provide different plasmon modes to be used in SEF [22–24]. The gap plasmon mode, originating from the close proximity of two or more metallic nanoparticles, has also been incorporated in SEF [25]. However, its regulation based on the traditional self-assembly technique has rarely been reported [26], since it calls for the fine tuning of the aggregation of the nanoparticles, which is practically challenging.

Here, a gap-plasmon tunable Ag bilayer nanoparticle film is demonstrated, where a variable number of polyelectrolyte (PEL) layers are sandwiched between two self-assembled silver nanoparticle layers. Compared to traditional monolayer metallic nanostructures, the presented Ag bilayer nanoparticle film exhibits some advantages. First, based on the self-assembly technique, the presented substrate is relatively homogeneous. Secondly, the surface density of the Ag nanoparticles is higher by using a second deposition, to meet the need of an effective SEF effect. Thirdly, the gap plasmon of the Ag nanoparticles from two different layers can be tuned across the visible spectral range by controlling the number of PEL interlayers, leading to the rational design of the substrate for SEF. Compared with a recent report on the similarly prepared gold bilayer nanoparticle film [27], the use of Ag herein enables a much larger tunable range. Using the experimentally observed optimal number of PEL interlayers, the presented substrate is subsequently applied to the fluorescence immunoassay. Compared to the control immunoassay where a glass substrate is used, an enhancement of approximately 3.3 fold in the signal intensity is obtained, indicating its potential application in immunoassays as well as other fluorescence-based assays.

Experimental Section

Materials

Poly (diallyldimethylammonium chloride) (PDDA), MW 100000-200000, Poly (sodium styrenesulfonate) (PSS), MW 70000, and poly (allylamide hydrochloride) (PAH) MW 15000 were obtained from Sigma-Aldrich. Silver nitrate was obtained from Shanghai Shenbo Chemical Co., Ltd. Trisodium citrate dihydrate was purchased from Jiangsu Qiangsheng Chemical Co., Ltd. Sodium tetraborate ($Na_2B_4O_7$) was purchased from Nanjing Chemical Co., Ltd. Poly-L-Lysine (PLL) was purchased from Beyotime Institute of Biotechnology. PLL-coated glass slides and Bovine serum albumin (BSA) were obtained from Nanjing KeyGEN Biotech. Co., Ltd. Human and mouse immunoglobulins (IgGs), and FITC labeled goat anti-human IgG (FITC-GAH IgG) were obtained from Beijing Bioss Biotech Co., Ltd. Polyoxyethylene (20) sorbitan monolaurate (Tween-20) and Tris (hydroxymethyl) aminomethane (TRIS) were obtained from Sinopharm Chemical Reagent Co., Ltd. TBS solution was prepared by dissolving NaCl (8.76 g) and TRIS (1.21 g) in water (500 mL). TBST solution was prepared by mixing Tween-20 (0.25 g) with TBS (500 mL). BBS solution was prepared by dissolving Sodium tetraborate in water to a concentration of 2 mM, reaching a pH of 9.0. The water used in the experiments was ultrapure deionized water.

Synthesis of Ag Nanoparticles

Ag nanoparticles were synthesized according to Lee's method [28]. Briefly, an aqueous solution of $AgNO_3$ (0.0849 g, 1 mM) was brought to boiling under stirring. After trisodium citrate solution (10 mL, 1 % w/w) was added, the mixture was boiled for 1 h under vigorous stirring and then allowed to cool slowly to room temperature. The as-prepared Ag nanoparticles were greenish yellow in color and characterized by an extinction peak at 406 nm.

Preparation of the Self-Assembled Ag Nanoparticle Monolayer Film

The glass slides were first treated with a 4:1 (v/v) mixture of H_2SO_4 (98 %) and H_2O_2 (30 %) at 60 °C for 6 h to remove the impurities and to activate the surface. After thoroughly rinsed with water, the glass slides were immersed in PDDA solution (1 %) for 20 min and then washed with water again. The PDDA-covered glass slides were then covered with black tapes containing punched holes (9 mm in diameter) to form wells on the surface of the slides. After that the slides were immersed in Ag solution for 8 h to form an Ag nanoparticle layer. The slides were rinsed thoroughly, dried under argon and stored under 4 °C until use.

Preparation of the Gap-Plasmon Tunable Ag Bilayer Nanoparticle Film

On the as-prepared Ag monolayer film, a layer-by-layer (LbL) process was conducted by the deposition of alternating layers of PAH and PSS, both of which were prepared at 2 mg mL^{-1} in 0.5 M NaCl solution and dissolved by sonication for 15 min. For the deposition of each layer, PEL solutions were pipetted into the wells on the slides at 100 μL/well and incubated for 15 min before being rinsed thoroughly with water. First, positively charged PAH was

deposited on the slides to be adsorbed on silver nanoparticles electrostatically. Then negatively charged PSS was deposited on the positively charged slide surface allowing for further PAH deposition. The top layer was always PAH in order for the assembly of a second Ag nanoparticle layer. After the deposition of a desired number of PEL layers, the slides were immersed in Ag solution again for 8 h before being rinsed thoroughly. For antigen immobilization in the immunoassays, an additional layer of PLL was deposited by pipetting the PLL solution (1 mg/mL) into the wells at 100 μL/well for an incubation time of 1 h. After being rinsed carefully, the slides were stored under 4 °C until use. A scheme of the presented Ag bilayer nanoparticle film is shown in Scheme 1.

SEF Activity Performance

FITC-GAH IgG (100 μg/mL in BBS) was added to the wells on Ag bilayer films, Ag monolayer films, and PLL-coated glass substrates, and then incubated overnight under 4 °C in a humid chamber. (The PLL-coated glass substrates were also covered with black tapes with holes as the Ag substrates for a quantitative comparison) After being rinsed with TBST, TBS and water for three times, the slides were dried under argon and stored under 4 °C until being measured.

Immunoassay Procedures

Immunoassays were performed on both Ag bilayer films and PLL-coated glass substrates. The IgG solutions were diluted with BBS. An aliquot of human IgG (100 μL) was added to each well. The slides were incubated overnight under 4 °C in a humid chamber, and then rinsed with TBST, TBS, and water for three times. Blocking was then performed by adding BSA solution (5 % in TBS, 100 μL) to each well and incubating in a humid chamber for 3 h under 37 °C. After the slides were rinsed with TBST and water, FITC-GAH IgG (100 μg/mL, 100 μL) was added to each well and then incubated for 1 h under 37 °C. Then the slides were thoroughly rinsed with TBST, TBS and water in sequence, dried under argon and stored under 4 °C until use.

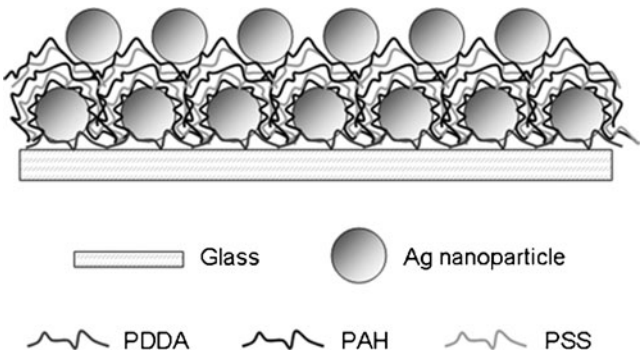

Scheme 1 The structure of the gap-plasmon tunable Ag bilayer nanoparticle film

Characterization

UV/Vis spectra were measured with a Shimadzu UV-3600 PC spectrophotometer. Aqueous samples were measured in quartz cuvettes of 1 cm path length, using pure water as a control. For samples on glass slides, the slides were placed in a direction such that the incident light beams were perpendicular to the slide surface. Fluorescence spectra were measured using an Edinburgh FLS 920 combined fluorescence lifetime and steady-state spectrometer. An excitation of 488 nm from the xenon lamp was used for measurements in front-face geometry, and fluorescence was detected on the same side of the slide. The power of the excitation at the sample surface and the illuminated sample area were measured to be around 0.17 mW and 7 mm^2, respectively. The integration time was set to 0.5 s. For measuring the dye-labelled IgG immobilized silver or glass slides, another slide similarly prepared but without dye-labelled IgG was used as a background control to eliminate the interference of the background noise.

SEM images characterizing the surface morphology of the Ag monolayer and bilayer films were taken with a scanning electron microscope (S-3000N).

Results and discussion

Characterization of the Novel Gap-Plasmon Tunable Ag Bilayer Nanoparticle Films

The surface morphology of the Ag monolayer nanoparticle film is shown in Fig. 1a, where a two-dimensional distribution of Ag nanoparticles is clearly exhibited. The as-prepared Ag nanoparticles are mostly spherical with an average diameter of around 50 nm. Although some samller particles and some rods also exist, the film is relatively homogeneous. Fig. 1b shows the case where a second Ag nanoparticle layer was deposited with 5 PEL layers in between. Some Ag nanoparticles can be observed to be located on top of the other particles, thus forming a nominal bilayer structure. The average distance between the two Ag layers was controlled by the number of the PEL interlayers, resulting in varied extinction spectra of the substrate, as shown in Fig. 2.

From Fig. 2, one can identify the extinction spectrum of the Ag monolayer substrate and the evolution of the extinction spectra of the Ag bilayer films with increasing PEL interlayers. The narrow SPR peak of Ag monolayer film at around 380 nm represents the dipolar mode, while the weak

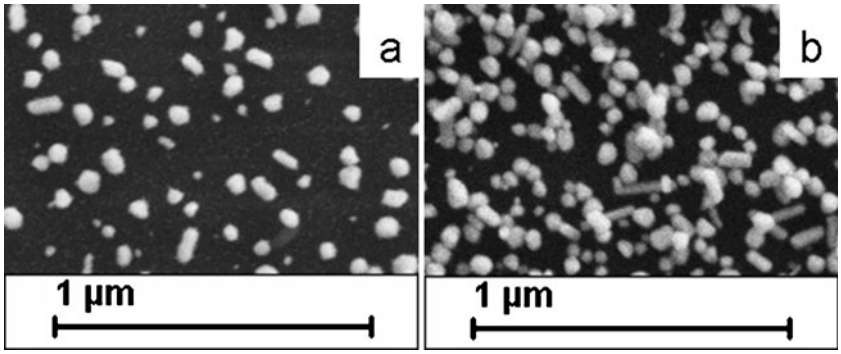

Fig. 1 SEM images of an Ag monolayer substrate (**a**) and an Ag bilayer substrate with 5 PEL interlayers (**b**)

broad band in the longer wavelength region suggests the appearance of the Ag nanoparticle aggregates formed during synthesis and deposition. For the Ag bilayer films, the extinction spectra are dominated by two peaks resulted from the split of the former dipolar mode sustained by isolated Ag nanoparticles, although the band due to intralayer aggregation still exits. While the shorter-wavelength band peaks at the similar spectral region with the Ag dipolar mode, the longer-wavelength band, which is referred to as the gap plasmon mode between the Ag nanoparticles from two different layers, is easily tunable with varying PEL interlayer numbers. When only one PAH interlayer was used, the peak of the gap plasmon mode appears at around 700 nm. As the PEL interlayer number increases, it blue shifts across almost the whole visible spectral range from about 700 nm to about 430 nm.

The shift of gap plasmon peak due to the distance change has been extensively studied, and can be well illustrated by the plasmon hybridization model [27, 29]. The control of the peak position, however, has rarely been performed due to the difficulties in controlling the aggregation of the nanoparticles in the traditional two dimensional manner. The method employed here, which regulates the gap plasmon of nanoparticles from two different layers by controlling the PEL interlayer number, is expected to provide new insights into the design of the substrate.

Determination of the Optimum Gap-Plasmon Tunable Ag Bilayer Nanoparticle Film for SEF

To examine and compare the SEF activities of the presented substrates, they were tested using FITC as the fluorophore. FITC labelled antibody were deposited on a PLL-coated glass substrate, a Ag monolayer film and the Ag bilayer films with different numbers of PEL interlayers, respectively, using the above described methods. The protein was used both as a fluorophore carrier and as a spacer to avoid the fluorescence quenching. [7] The results are shown in Fig. 3.

According to Fig. 3, fluorescence enhancements were obtained on all the substrates deposited with silver nanoparticles. The Ag monolayer film exhibits an enhancement of around 6.5 fold over the PLL-coated glass substrate. For the bilayer films, there is a clear trend of fluorescence enhancement variation that first increases and then decreases with a maximal enhancement of around 15.4 fold achieved with 7 PEL interlayers. The significant fluorescence variation

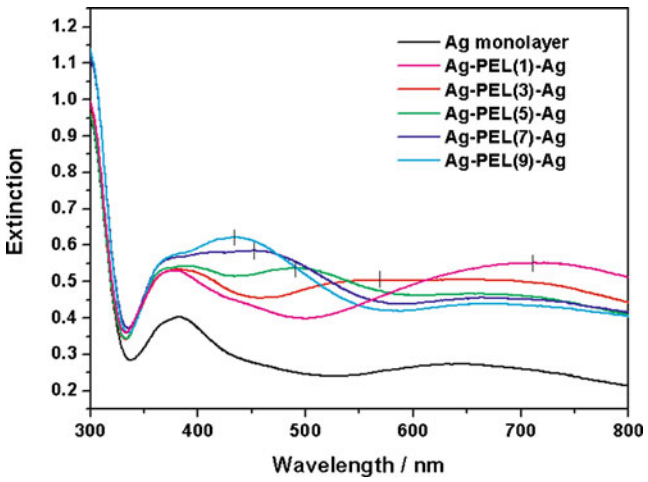

Fig. 2 Extinction spectra of the Ag monolayer film (*black*) and Ag bilayer films with 1 (*violet*), 3 (*red*), 5 (*green*), 7 (*blue*) and 9 (*cyan*) PEL interlayers

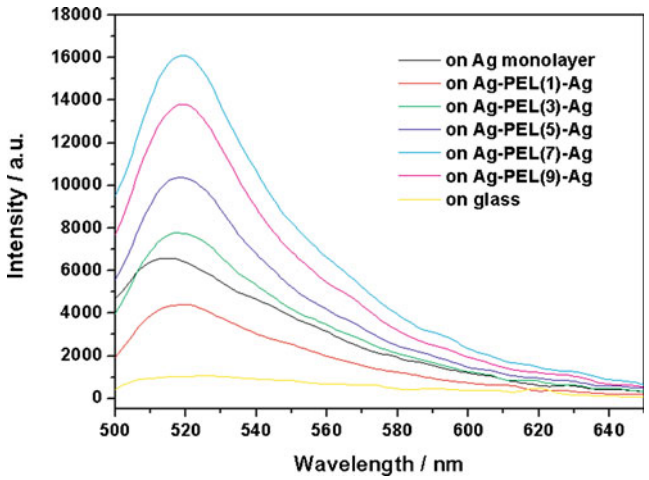

Fig. 3 Fluorescence spectra of FITC-GAH IgG immobilized on the Ag monolayer substrate (*black*), Ag bilayer substrates with 1 (*red*), 3 (*green*), 5 (*blue*), 7 (*cyan*) and 9 (*violet*) PEL interlayers, as well as on the PLL-coated glass substrate (*yellow*)

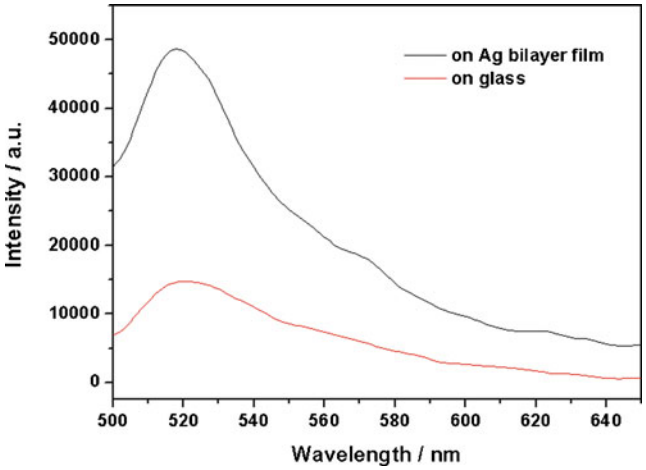

Fig. 4 Comparison of the immunoassay fluorescence emission measured on an optimized gap-plasmon tunable Ag bilayer nanoparticle film (*black*) and a PLL-coated glass slide (*red*)

observed can not be accounted for by the changes of the surface density of Ag nanoparticles alone, because it changes little with the increasing PEL interlayers (data not shown). Moreover, as the number of the PEL interlayers increased, the interaction between the two Ag nanoparticle layers decreased, leading to a weaker electromagnetic field between the Ag nanoparticles, which could not explain the observed fluorescence enhancement. Consequently, other mechanisms are considered to be involved besides the geometrical ones.

Although the exact mechanism is still under debate, SEF is considered to be strongly dependent on the SPR properties of the substrates [22]. Either the enhanced excitation field or the enhanced emission, or both of the above two may contribute to the total enhancement, depending on the SPR peak position relative to the absorption and emission spectra of the fluorophore as well as the excitation wavelength [30–32]. In the present experiment, as the wavelength difference between the excitation and the emission is relatively small, it is most probable that the observed fluorescence enhancement comes from both the excitation and the emission processes, whose contributions, however, may change with the different SPR peak position of the substrate, making the total enhancement varied. SPR peak position changes are consequently considered to be responsible for the changes of the enhancement, demonstrating the potential of our gap-plasmon tunable Ag bilayer nanoparticle films in regulating the SEF effect.

Enhanced Fluorescence Immunoassays

The fluorescence spectra obtained from the immunoassays performed on our Ag bilayer nanoparticle film with 7 PEL interlayers and a PLL-coated glass substrate are shown in Fig. 4. An enhancement of approximately 3.3 fold was observed without obvious change in the profile compared to the non-enhanced sample, which is consistent with previous reports [33]. The enhancement factor obtained here is significantly smaller than that obtained previously in Section 3.2. The reasons are analyzed as follows. Compared to the SEF activity test using FITC-GAH IgG immobilized on the bare Ag bilayer nanoparticle films, an additional layer of PLL was deposited on the substrates before the immunoassay in order to improve the specificity. Moreover, instead of direct immobilization, FITC-GAH IgG was attached to the surface-bound human IgG after BSA blocking in the immunoassay. Consequently, the average distance between the fluorophores and the metallic nanoparticle surfaces becomes larger. In a rough estimation of the geometrical dimensions, the thickness of PLL is around 1.5 nm, the size of a BSA molecule is 5–11 nm [24], and the IgGs used here are 10–20 nm in size [34–36]. Assuming a random distribution of the FITC molecules on the antibodies, the average distance between the fluorophores and the metallic nanoparticle surfaces is within 11.5–31.5 nm in the immunoassay, compared to an average distance of 5–10 nm in the case

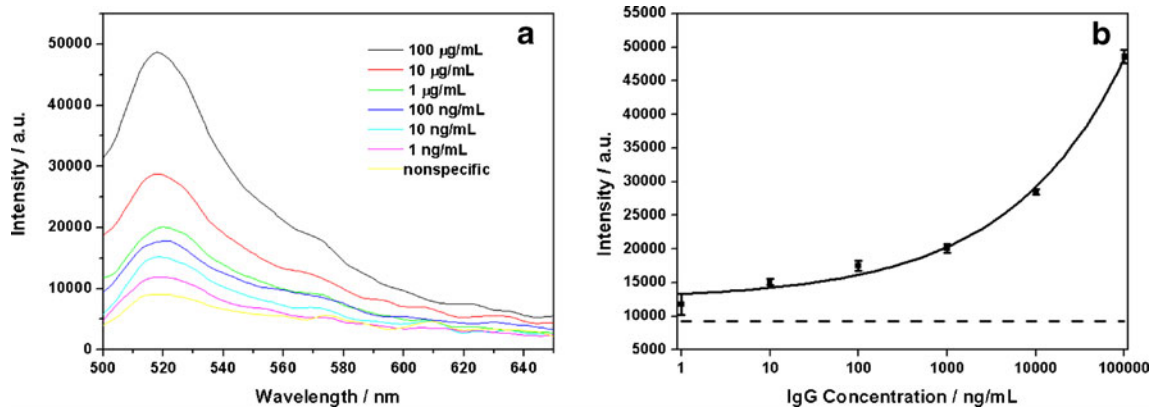

Fig. 5 **a** Immunoassay fluorescence emission measured on the optimal gap-plasmon tunable Ag bilayer nanoparticle films using human IgG with different concentrations. **b** Calibration curve of the fluorescence signal vs. the concentration of human IgG (*solid*), corresponding to (**a**). The *dashed line* represents the level of nonspecific binding

of direct immobilization. According to the strongly distance-dependent nature of SEF as well as previous reports on the optimal distance [5–8], the decreased enhancement factor is considered to be logical. However, by modifying some key factors that affect SEF, e.g., the nanoparticle size [21], the enhancement factor can be further optimized.

In addition to the fluorescence enhancement, the ability of our Ag bilayer nanoparticle film in the analytical performance of immunoassays was demonstrated using human IgG. A direct assay format was used in which human antigen with different concentrations was directly immobilized on the substrates followed by the immune reaction with the labelled antibody. The corresponding fluorescence spectra are shown in Fig. 5a. When a concentration of 100 μg/mL was used for the human antigen, a fluorescence spectrum with the peak intensity of around 50000 counts was obtained. As the concentration of the human antigen decreased, the fluorescence intensity also decreased, to approximately 1200 counts for a concentration of 1 ng/mL. Unfortunately the further decrease of the resolvable concentration was hindered by the weak background of the nonspecific binding. The calibration curve for the enhanced immunoassays was also depicted accordingly, as shown in Fig. 5b. The data were fitted well using an exponential logistic plot and the background signal level is also depicted by a dashed line. It is thus concluded that using the presented gap plasmon-tunable Ag bilayer nanoparticle film, the fluorescence immunoassay can be performed with enhanced fluorescence signals. The limit of detection (LOD) is as low as 1 ng/mL.

Conclusions

A novel gap-plasmon tunable Ag bilayer nanoparticle film, consisting of two layers of self-assembled Ag nanoparticles and a variable number of PEL layers in between, is developed. By controlling the number of the PEL interlayers, the gap plasmon mode of the Ag nanoparticles from two different layers can be tuned across the visible spectral range conveniently. The ability of the substrate in fluorescence enhancement was examined experimentally, where the enhancement factor was found to first increase and then decrease with the increasing PEL interlayer numbers. A maximum enhancement was achieved with 7 PEL interlayers. Subsequently, this experimentally determined optimal substrate was employed in fluorescence immunoassays. An enhancement of approximately 3.3 fold in fluorescence intensity was obtained, compared to that obtained on a traditional glass substrate. The experimental results presented herein suggest that the developed gap-plasmon tunable Ag bilayer nanoparticle film is potentially useful in SEF-based immunoassays, which provides new insights into the rational design of the SEF substrates.

Acknowledgement This work was supported by the Natural Science Foundation of China (NSFC) (Nos. 60708024, 60877024), and Specialized Research Fund for the Doctoral Program of Higher Education (SRFDP) (Nos. 20070286058, 20090092110015).

References

1. Gosling JP (1990) A decade of development in immunoassay methodology. Clin Chem 36(8):1408–1427
2. Aslan K, Gryczynski I, Malicka J, Matveeva E, Lakowicz JR, Geddes CD (2005) Metal-enhanced fluorescence: an emerging tool in biotechnology. Curr Opin Biotechnol 16(1):55–62. doi:10.1016/j.copbio.2005.01.001
3. Li RQ, Xu SH, Wang CL, Shao HB, Xu QY, Cui YP (2010) Metal-enhanced fluorescence of CdTe nanocrystals in aqueous solution. Chemphyschem 11(12):2582–2588. doi:10.1002/cphc.201000239
4. Zhang RH, Wang ZY, Song CY, Yang J, Li J, Sadaf A, Cui YP (2011) Surface-enhanced fluorescence from fluorophore-assembled monolayers by using Ag@SiO_2 nanoparticles. Chemphyschem 12(5):992–998. doi:10.1002/cphc.201000849
5. Kulakovich O, Strekal N, Yaroshevich A, Maskevich S, Gaponenko S, Nabiev I, Woggon U, Artemyev M (2002) Enhanced luminescence of CdSe quantum dots on gold colloids. Nano Lett 2(12):1449–1452. doi:10.1021/nl025819k
6. Malicka J, Gryczynski I, Gryczynski Z, Lakowicz JR (2003) Effects of fluorophore-to-silver distance on the emission of cyanine-dye-labeled oligonucleotides. Anal Biochem 315(1):57–66. doi:10.1016/s0003-2697(02)00702-9
7. Anger P, Bharadwaj P, Novotny L (2006) Enhancement and quenching of single-molecule fluorescence. Phys Rev Lett 96 (11). doi:10.1103/PhysRevLett.96.113002
8. Wang YS, Liu B, Mikhailovsky A, Bazan GC (2010) Conjugated polyelectrolyte-metal nanoparticle platforms for optically amplified DNA detection. Adv Mater 22(5):656–659. doi:10.1002/adma.200902675
9. Lakowicz JR, Shen YB, D'Auria S, Malicka J, Fang JY, Gryczynski Z, Gryczynski I (2002) Radiative decay engineering 2. Effects of silver island films on fluorescence intensity, lifetimes, and resonance energy transfer. Anal Biochem 301(2):261–277. doi:10.1006/abio.2001.5503
10. Gersten J, Nitzan A (1981) Spectroscopic properties of molecules interacting with small dielectric particles. J Chem Phys 75 (3):1139–1152. doi:10.1063/1.442161
11. Ruppin R (1982) Decay of an excited molecule near a small metal sphere. J Chem Phys 76(4):1681–1684. doi:10.1063/1.443196
12. Das PC, Puri A (2002) Energy flow and fluorescence near a small metal particle. Phys Rev B 65(15). doi:10.1103/PhysRevB.65.155416
13. Sokolov K, Chumanov G, Cotton TM (1998) Enhancement of molecular fluorescence near the surface of colloidal metal films. Anal Chem 70(18):3898–3905. doi:10.1021/ac9712310
14. Hayakawa T, Selvan ST, Nogami M (1999) Field enhancement effect of small Ag particles on the fluorescence from Eu^{3+}-doped SiO_2 glass. Appl Phys Lett 74(11):1513–1515. doi:10.1063/1.123600
15. Selvan ST, Hayakawa T, Nogami M (1999) Remarkable influence of silver islands on the enhancement of fluorescence from Eu^{3+} ion-doped silica gels. J Phys Chem B 103(34):7064–7067. doi:10.1021/jp9902755
16. Lakowicz JR (2005) Radiative decay engineering 5: metal-enhanced fluorescence and plasmon emission. Anal Biochem 337(2):171–194. doi:10.1016/j.ab.2004.11.026
17. Matveeva EG, Gryczynski Z, Lakowicz JR (2005) Myoglobin immunoassay based on metal particle-enhanced fluorescence. J Immunol Methods 302(1–2):26–35. doi:10.1016/j.jim.2005.04.020

18. Zhang J, Matveeva E, Gryczynski I, Leonenko Z, Lakowicz JR (2005) Metal-enhanced fluoroimmunoassay on a silver film by vapor deposition. J Phys Chem B 109(16):7969–7975. doi:10.1021/jp0456842
19. Shtoyko T, Matveeva EG, Chang IF, Gryczynski Z, Goldys E, Gryczynski I (2008) Enhanced fluorescent immunoassays on silver fractal-like structures. Anal Chem 80(6):1962–1966. doi:10.1021/ac7019915
20. Barnett A, Matveeva EG, Gryczynski I, Gryczynski Z, Goldys EM (2007) Coupled plasmon effects for the enhancement of fluorescent immunoassays. Physica B 394(2):297–300. doi:10.1016/j.physb.2006.12.085
21. Nooney R, Clifford A, LeGuevel X, Stranik O, McDonagh C, MacCraith BD (2010) Enhancing the analytical performance of immunoassays that employ metal-enhanced fluorescence. Anal Bioanal Chem 396(3):1127–1134. doi:10.1007/s00216-009-3357-9
22. Tam F, Goodrich GP, Johnson BR, Halas NJ (2007) Plasmonic enhancement of molecular fluorescence. Nano Lett 7(2):496–501. doi:10.1021/nl062901x
23. Chen Y, Munechika K, Ginger DS (2007) Dependence of fluorescence intensity on the spectral overlap between fluorophores and plasmon resonant single silver nanoparticles. Nano Lett 7(3):690–696. doi:10.1021/nl062795z
24. Bardhan R, Grady NK, Cole JR, Joshi A, Halas NJ (2009) Fluorescence enhancement by Au nanostructures: nanoshells and nanorods. ACS Nano 3(3):744–752. doi:10.1021/nn900001q
25. Ishida A, Kumagai K (2009) Fluorescence enhancement due to gap mode of gold colloids immobilized on a hydrophilic amino-terminated glass substrate. Chem Lett 38(2):144–145. doi:10.1246/cl.2009.144
26. Lu Y, Liu GL, Lee LP (2005) High-density silver nanoparticle film with temperature-controllable interparticle spacing for a tunable surface enhanced Raman scattering substrate. Nano Lett 5(1):5–9. doi:10.1021/nl048965u
27. Cunningham A, Muhlig S, Rockstuhl C, Burgi T (2011) Coupling of Plasmon Resonances in Tunable Layered Arrays of Gold Nanoparticles. J Phys Chem C 115(18):8955–8960. doi:10.1021/jp2011364
28. Lee PC, Meisel D (1982) Adsorption and surface-enhanced raman of dyes on silver and gold sols. J Phys Chem 86(17):3391–3395. doi:10.1021/j100214a025
29. Nordlander P, Oubre C, Prodan E, Li K, Stockman MI (2004) Plasmon hybridization in nanoparticle dimers. Nano Lett 4 (5):899–903. doi:10.1021/nl049681c
30. Kuhn S, Hakanson U, Rogobete L, Sandoghdar V (2006) Enhancement of single-molecule fluorescence using a gold nanoparticle as an optical nanoantenna. Phys Rev Lett 97(1). doi:10.1103/PhysRevLett.97.017402
31. Viste P, Plain J, Jaffiol R, Vial A, Adam PM, Royer P (2010) Enhancement and quenching regimes in metal–semiconductor hybrid optical nanosources. ACS Nano 4(2):759–764. doi:10.1021/nn901294d
32. Ming T, Zhao L, Yang Z, Chen HJ, Sun LD, Wang JF, Yan CH (2009) Strong polarization dependence of plasmon-enhanced fluorescence on single gold nanorods. Nano Lett 9(11):3896–3903. doi:10.1021/nl902095q
33. Aslan K, Lakowicz JR, Geddes CD (2005) Metal-enhanced fluorescence using anisotropic silver nanostructures: critical progress to date. Anal Bioanal Chem 382(4):926–933. doi:10.1007/s00216-005-3195-3
34. Hogendoorn PCW, Vandorst EBL, Vanderburg SH, Bruijn JA, Daha MR, Hoedemaeker PJ, Fleuren GJ (1993) Antigen size influences the type of glomerular pathology in chronic serum sickness. Nephrol Dial Transplant 8(8):703–710
35. Caruso F, Furlong DN, Ariga K, Ichinose I, Kunitake T (1998) Characterization of polyelectrolyte-protein multilayer films by atomic force microscopy, scanning electron microscopy, and Fourier transform infrared reflection-absorption spectroscopy. Langmuir 14(16):4559–4565. doi:10.1021/la971288h
36. Lv Z, Wang JH, Chen GP, Deng LH (2011) Imaging and determining friction forces of specific interactions between human IgG and rat anti-human IgG. J Biol Phys 37(4):417–427. doi:10.1007/s10867-011-9223-y